



Probing drug-cell interactions

Over the past two decades, the subset of scanning probe microscopy termed atomic force microscopy (AFM) has become a ubiquitous tool to image nanoscale structure and to estimate certain mechanical characteristics of biological entities ranging from DNA to tissues. Various modes of imaging and force spectroscopies have been developed to correlate structure, properties, and chemomechanical interactions of molecules and cells in aqueous environments. These advances in AFM have led rapidly to *in situ* investigations of drug-induced changes in cell structure, membrane stability, and receptor interaction forces.

Krystyn J. Van Vliet¹ and Peter Hinterdorfer²

¹Department of Materials Science and Engineering, Massachusetts Institute of Technology, 77 Massachusetts Avenue, Room 8-237, Cambridge, MA 02139 USA

E-mail: krystyn@mit.edu

²Institute for Biophysics, Johannes Kepler Universität Linz, Altenbergerstr. 69, A-4040, Linz, Austria

E-mail: peter.hinterdorfer@jk.uni-linz.ac.at

The AFM was originally developed as an adaptation of another scanning probe microscopy technology, the scanning tunneling microscope, to image nonconductive materials through direct physical contact between a cantilevered probe and a sample surface¹. Although not originally conceived to image biological structures, the researchers who developed this tool quickly recognized that the piconewton-scale force and nanometer-scale displacement resolutions of the AFM enable the topographical scanning of mechanically compliant materials, including biological structures in aqueous environments. Haberle *et al.* introduced this approach as 'underwater AFM' and demonstrated the capacity to image changes in the structure and topography of capillary-bound red blood cells as a function of hypotonicity and after binding of antibodies. They modestly suggest that this approach enables

in situ study of a range of dynamics at the surface of living cells². Current research underscores the significance of this invention, as an increasing array of imaging and force spectroscopy modes have been developed to exploit this simple concept: intermolecular forces can be measured directly and can also be harnessed to image a macromolecular structure with subnanometer spatial resolution.

The operating principles of all AFMs include three key features, as shown in Fig. 1a: a reflective, cantilevered probe; a laser-photodiode-piezocrystal feedback loop that maintains either constant deflection or oscillation amplitude of the cantilever through displacement of the cantilever base in the vertical plane; and a piezo-actuated scanner that translates either the cantilever or the sample in the horizontal plane. Several modifications to the basic imaging modalities (constant contact

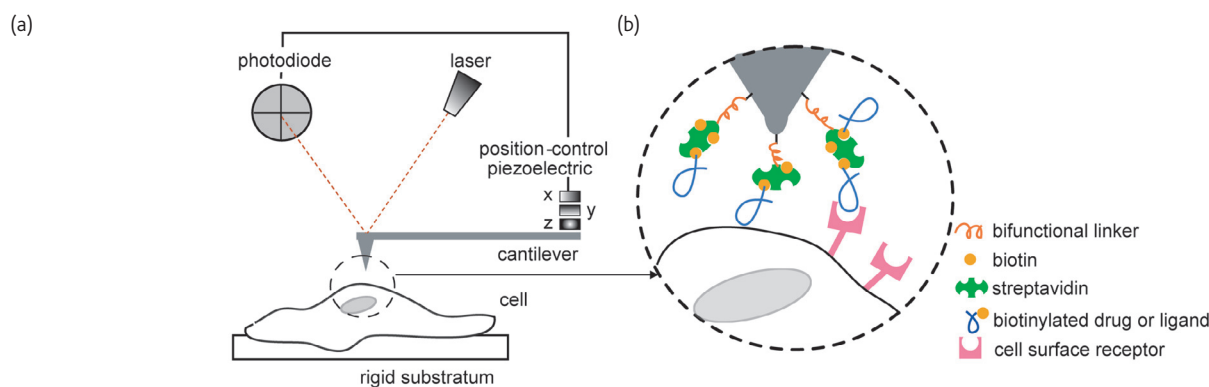


Fig. 1 Schematic of AFM principal components (a) and probe functionalization approaches to quantify intermolecular forces between surfaces such as individual drugs or molecular ligands and cell surface receptors (b). (Adapted from⁷³. Reprinted with permission. © 2003 Elsevier.)

mode, or iso-force imaging; and dynamic contact mode, or iso-amplitude imaging) enhance the resolution of hydrated biological structures in fluid and enable direct measurement of intermolecular binding (e.g. electromagnetic oscillation of the free-end of magnetically coated cantilevers, termed MAC mode³). As in all scanning probe microscopies, images comprise rastered lines of pixels, and acquired signals are represented as image contrast. Topography or height images indicate micron-scale displacement of the cantilever base. Deflection images indicate the nanoscale error signal in the contact mode iso-force feedback loop, and typically provide impressive image contrast for mechanically heterogeneous structures such as living cells. Amplitude images indicate the error signal in the iso-amplitude feedback loop and are indicative of energy absorption. Phase images indicate the phase lag between the cantilever base and free-end and are also indicative of energy absorption. The interpretation of these images in terms of mechanical properties is an area of active research⁴⁻⁶. The independent control of cantilever displacement normal to the sample surface also enables force spectroscopy, the measurement of the force-displacement response resulting from contact at discrete points on the sample surface and/or extension of a biomacromolecule that is chemically adhered to the cantilever and the sample surface. These chemomechanical interactions can be obtained during scanning in various modes to acquire mechanical and binding force concurrently with topography⁷, and relate directly to local mechanical properties^{8,9} and intermolecular binding kinetics¹⁰.

Time-lapsed imaging and force spectroscopy afforded by environmentally controlled AFM has led to significant progress in probing the mechanisms by which biological and synthetic chemicals, including therapeutic drugs, interface with and modify the structure and function of individual living cells in real time. The drug-cell interactions studied cover a wide range of fields and objectives, but the majority of these applications seek to clarify the dynamics of structural adaptations within the cell that correlate with mechanical functions such as motility, reorganization of the cell membrane that serves as the interface between the cell and the extracellular environment, and characterization

of the binding between drugs – here, considered naturally occurring and synthetic therapeutic reagents – to cell surface receptors that induce new metabolic responses. Here, we present an overview of this emerging field, as enabled by direct measurement and analysis of the nanomechanical interactions between molecules.

Structural dynamics

The earliest reported and most common consideration of drug-cell interactions is in terms of structural adaptations of the whole cell and the intracellular structures of mammalian cells that are adherent, meaning that these cells attach readily to solid surfaces. This mechanical imaging of cell response to drugs that induce morphological differentiation, such as retinoic acid induction of neuroblastoma cells¹¹, or that cause disruption of cytoskeletal networks, such as cytochalasin-D disintegration of cytoskeletal actin¹², was initially considered as a complement to optical microscopy approaches that could provide the same structural information at lower spatial resolution (~400 nm). However, the additional understanding of drug mechanisms afforded by mechanical probing of cells was soon recognized, and discrete indentation force-displacement ($F-d$) responses were analyzed to estimate the mechanical compliance of cells in response to drugs targeting different components of the cytoskeleton¹³⁻¹⁶. In such studies, cells (or at least the probed volumes of the cells) are assumed to act as a linear elastic material that is thick compared to the contact depth d , and an effective elastic modulus is inferred from the Hertzian elastic solution for a sphere ($F \propto Ed^{3/2}$) or a cone ($F \propto Ed^2$) depending on the cantilevered probe geometry. Fig. 2 illustrates the mechanical consequence of drug-induced disruption of the cytoskeletal network over time, where E is estimated for each pixel of the image. This approach is not appropriate for rapid structural or mechanical adaptations because of the timescale of such experiments. Imaging speed of a single cell of image size and resolution comparable to Fig. 1a is limited not by the instrument, but by the fragility of the cells, and requires <5 min/image. However, the individual $F-d$ acquisitions required to construct Figs. 1b and c require on the order of 1 s/pixel and

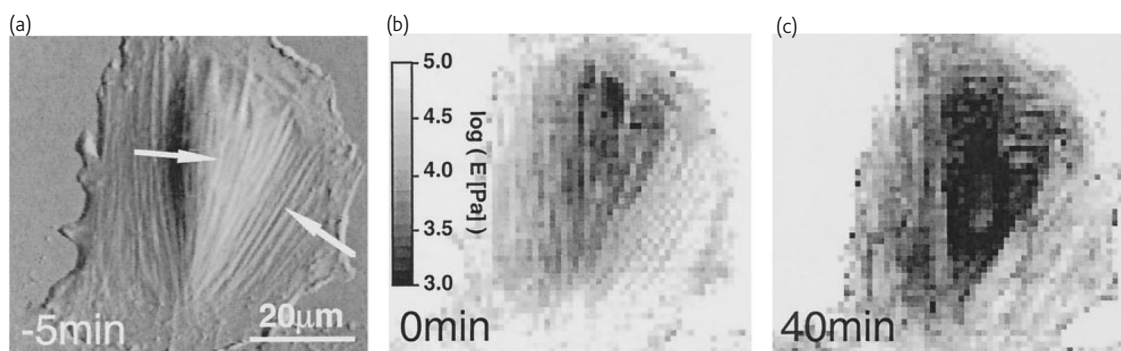


Fig. 2 Increased compliance of NRK fibroblast cells induced by cytoskeletal protein agonists. (a) Deflection or contact-mode error signal image before introduction of 10 mM cytochalasin D; arrows indicate filamentous-actin stress fibers. Effective indentation elastic modulus E for discrete points along the cell at the time at which this drug is introduced (b) and 40 min post-exposure (c) indicate that disintegration of actin networks correlates directly with increased compliance of the cell. (Reprinted with permission from¹⁵. © 2000 The Biophysical Society.)

thus >10 min/image, a throughput which decreases directly with increasing image resolution.

The structural adaptations induced by naturally occurring soluble biomolecules is equally valuable, especially when such lipo- and glycoproteins are possible catalysts for pathologies such as Alzheimer's disease¹⁷, HIV¹⁸, and cancers¹⁹, and therefore candidate targets for new drugs. As demonstrated by Rotsch *et al.*¹⁹ in Fig. 3, so-called growth factors can alter not just the morphology of cancer cell lamellipodia, but also the mechanical compliance of these structures. Such correlations enable testable hypotheses of how cells move, generate, and respond to force (mechanobiology²⁰), and can also clarify how drugs affect cell behavior at the functional level²¹. For example, Fig. 4 illustrates direct measurement of increased cell volume for adhered vascular endothelial cells in response to the hormone aldosterone, and reversal of this effect upon the addition of spironolactone, a potential drug to inhibit vasculopathy or abnormal swelling of capillaries²²⁻²⁴. Imaging of drug-induced structural dynamics within and between cells in this way is particularly well suited to the study of antibiotic effects on bacteria²⁵⁻²⁸, as these cells are significantly smaller than adherent mammalian cells

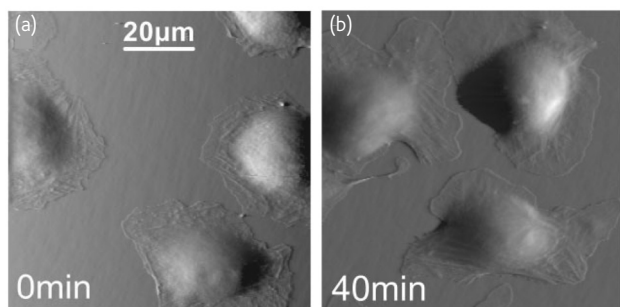


Fig. 3 Deflection or contact-mode error signal images and corresponding force-displacement responses of cancer cells (adenocarcinoma) demonstrate that 5 nM of epithelial growth factor, a naturally occurring protein secreted by tumor cells, induces extension and increased elastic compliance of lamellipodia. This structural/mechanical observation supports the hypothesis that the force generated by the lamellipodia of metastatic tumor cells is due in part to gel-swelling when actin networks are biochemically severed. (Reprinted with permission from¹⁹. © 2001 Elsevier.)

for which function is increasingly appreciated to depend on both chemical and mechanical cues^{29,30}.

Membrane dynamics

As the cell membrane is the physical and functional interface between the extracellular cues and intracellular genetic machinery that modifies cell function, the dynamics of the cell surface and physical models of this surface in response to soluble drugs or drug delivery vehicles are of keen interest. Pelling *et al.*³¹ measured the mechanical oscillations of the yeast cell wall as a function of temperature to estimate the required activation energy of such oscillations (Fig. 5). From the absence of these periodic fluctuations in the presence of sodium azide, a potent inhibitor of adenosine triphosphate (ATP) synthesis within the cell, the authors

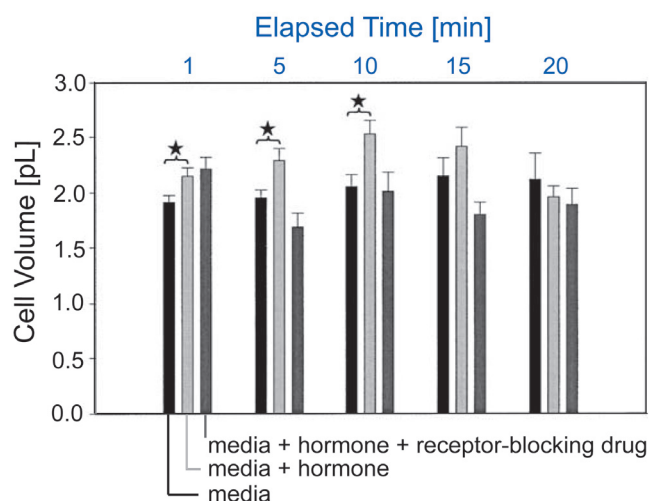


Fig. 4 Three-dimensional topology enables testing of hypotheses regarding drug mechanisms, without idealization of cell shape. Human umbilical vein endothelial cells swell within 1 min post-exposure to soluble aldosterone, a hormone. Stars indicate significant difference in mean values. This swelling is inhibited by the addition of the drug spironolactone, which blocks intracellular receptors, indicating that spironolactone is a possible therapy to prevent capillary swelling that restricts blood flow during inflammation. (Reprinted with permission from²². © 2003 Springer.)

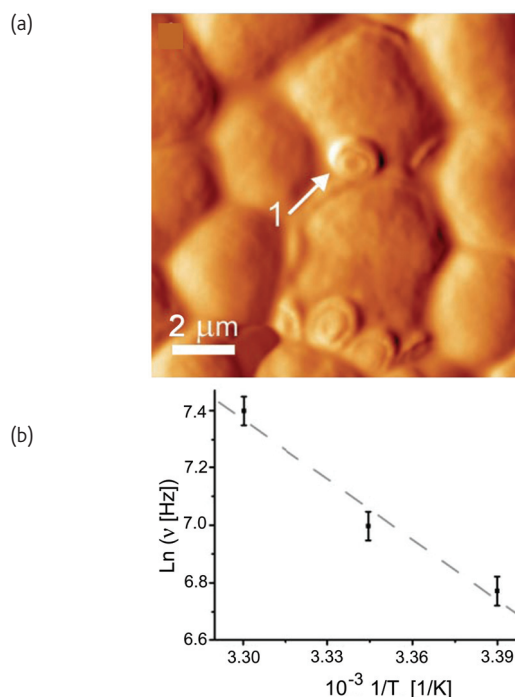


Fig. 5 Direct measurement of cell membrane mechanical oscillations allows consideration of how intracellular mechanosensory proteins are affected by drugs. (a) Deflection or contact-mode error signal image of dead yeast cells adsorbed to mica. Arrow indicates rigid bud scar. (b) Sustained acquisition of the force-displacement response at individual points on living yeast cell walls indicates a temperature-dependent oscillation frequency with activation energy of ~ 58 kJ/mol, consistent with that of molecular motor proteins such as myosin. These oscillations are absent in the presence of sodium azide, which inhibits production of the ATP required by molecular motor proteins. (Reprinted with permission from³¹. © 2004 American Association for the Advancement of Science.)

inferred that these membrane dynamics were the result of ATP-dependent molecular motor proteins such as myosin³¹.

Nonadherent cells such as erythrocytes and lymphocytes must be adhered to rigid substrata in order to analyze them using AFM, and therefore results should be interpreted with caution^{32,33}. However,

Girasole *et al.*³⁴ demonstrate that certain membrane characteristics of erythrocytes are not compromised by this gross change in cell shape, and that membrane undulations characteristic of certain pathologies can be induced by drugs to study the root causes, time course, and possible treatments of such diseases (Fig. 6).

The development of materials for drug³⁵⁻⁴⁰ and gene⁴¹ delivery into cells and cell nuclei requires understanding of how such vehicles interact with the cell membrane, for which time-lapse analysis of membrane dynamics is key^{37,42}. Through a combination of AFM and confocal optical microscopy, Almofti *et al.*³⁶ identified the charge ratio of lipids required to produce lipid-DNA complexes (lipoplexes) that were efficiently incorporated within the cell through direct fusion with the cell membrane (Figs. 7a-c). Shahin *et al.*⁴³ subsequently demonstrated that the dilation of pore complexes on the nuclear membrane – as may be required of efficient drug or gene delivery – is rapidly induced by the steroid dexamethasone (Fig. 7d). Others have demonstrated nuclear pore dynamics in response to different drugs^{44,45}. Considering model and isolated cell membranes, Hong *et al.*⁴⁶ demonstrated how dendrimers considered as candidate gene delivery vehicles can induce pore formation of certain phospholipid regions, which may be further developed as a mechanism for gene uptake or mitigated if such porosity compromises cell survival (Fig. 7e). Indeed, the spatial and temporal resolution afforded by AFM imaging provides access to the kinetics of such membrane reorganization in response to drugs, at least in lipid bilayer models adhered to rigid substrata (Fig. 8)^{47,48}.

Cell surface receptor interactions

Certainly, the most basic level of drug-cell interaction is at the intermolecular level, and nanomechanical measurement and *in situ* analysis of such ligand-receptor and antigen-antibody binding provides an unparalleled opportunity to study this initiation of the drug response in living cells. Here, force spectroscopy between molecular pairs can be measured at the single molecule level. For simplification, we will refer to the ligand as the probe-bound molecule, and the receptor as the molecule presented at the sample surface; strictly, a ligand is a molecule

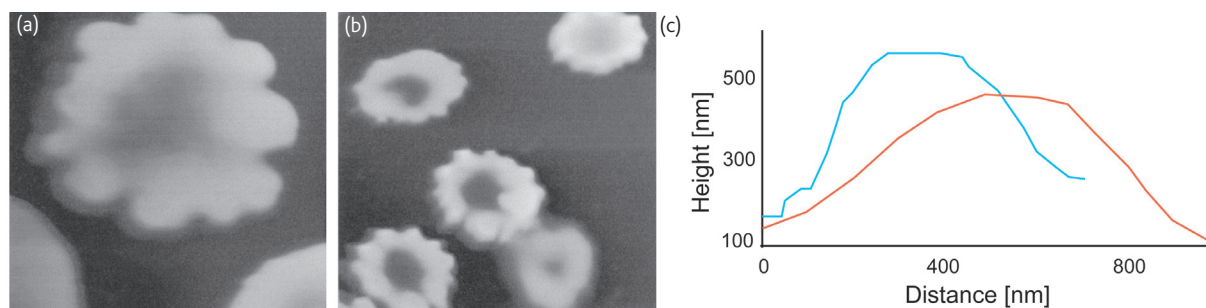


Fig. 6 Drug-induced correlations with membrane morphology of diseased cells can be investigated with limited success in cells that are not adherent *in vivo*, such as erythrocytes (red blood cells). Height images of erythrocytes from human patients with (a) the pathology, anisopoichilocytosis; and (b) no pathology, but incubated with 2 mg/mL lecithin show similar spicule formation. Cell diameter ~ 7 μm. (c) Three-dimensional topology of individual membrane protrusions indicates statistical difference in morphology when induced via >2 mg/mL lecithin (blue) or via 200 μL chlorprozamine in hypotonic media (red). (Reprinted with permission from³⁴. © 2001 Blackwell.)

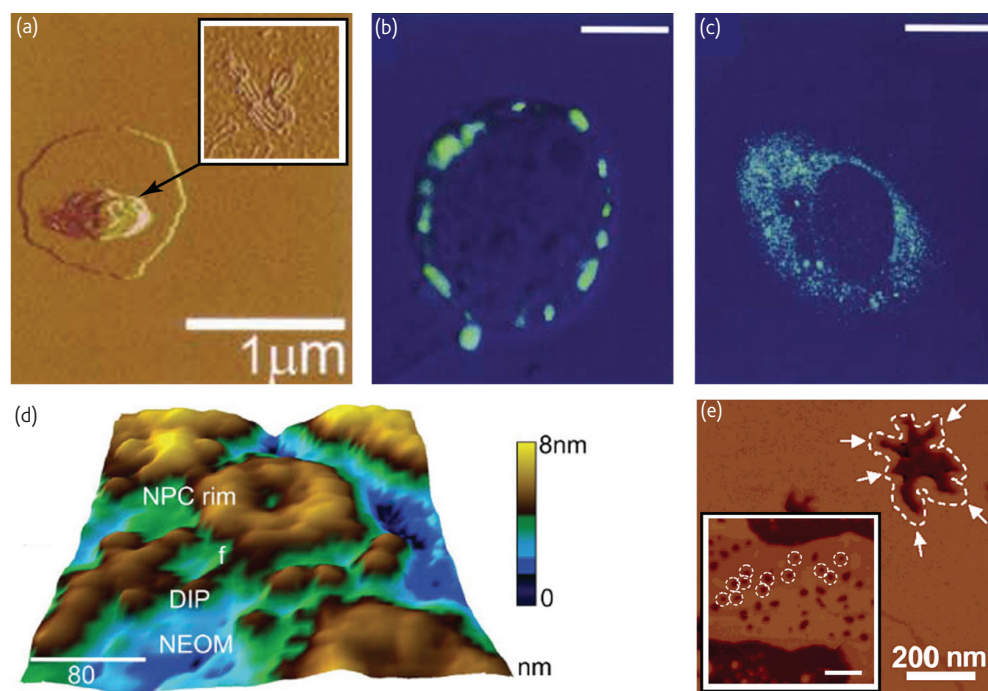


Fig. 7 Characterization of drug and gene delivery vehicles and mechanisms enhances vehicle development. (a) Deflection or contact-mode error signal image of lipoplex, a liposome containing DNA (DNA image, inset). Confocal optical microscopy of cells transfected with these lipoplexes for 1 h show the lipoplexes are constrained near the cell membrane in the presence of endocytosis inhibitors (b), whereas cells transfected in the presence of membrane fusion inhibitors do not show such localization (c). Scalebars in (b) and (c) = 10 μ m. This study identified the charge ratio required for internalization of lipoplexes for gene delivery. (d) Pores in nuclear membranes (NPCs) are dilated upon exposure to the steroid dexamethosone via induction of protein synthesis (DIP). NEOM is the nuclear envelope outer membrane. Scalebar = 80 nm. (e) Height image of lipid bilayers, representative of cell membranes, show that drug delivery via poly(amidoamine) dendrimers induces ~30 nm-diameter holes that grow via removal of lipids from the initial defect area (arrows). Inset scalebar = 200 nm. (Parts (a), (b), and (c) reprinted with permission from³⁶. © 2003 Elsevier. Part (d) reprinted with permission from⁴³, © 2005 Wiley.)

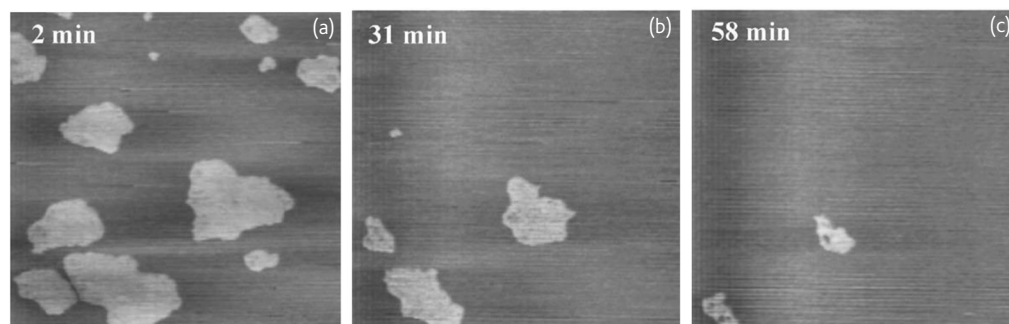


Fig. 8 As model cell membranes, lipid bilayers indicate kinetics of membrane reorganization in response to drugs. Time-lapse height images in constant-deflection mode of a choline phospholipid bilayer comprising DPPC (dipalmitoylphosphatidylcholine, gel phase) and DOPC (dioleoylphosphatidylcholine, fluid phase) on mica show rapid dissolution of the gel phase upon exposure to azithromycin, indicating reduced membrane stability in response to this drug. 7.5 μ m \times 7.5 μ m image size, with grayscale white corresponding to a height of 10 nm. (Reprinted with permission from⁴⁸. © 2004 Elsevier.)

that induces a biochemical response by binding specifically to another molecule, its receptor, via various mechanisms such as change in receptor conformation. A pharmaceutical drug can comprise a portion of a naturally occurring ligand, or an entire antibody that inhibits ligand binding to the intended receptor.

There are several potential advantages of such direct visualization and quantification of drug binding to intact cell surfaces. Firstly, receptor distribution can be mapped with spatial resolution superior to that afforded by immunocytochemical staining (fluorophore-labeled

antibodies), and can be directly correlated with structural and mechanical subcellular features such as cytoskeletal filament association. Secondly, the receptor locations are determined without permanent occlusion of the receptor, enabling time-lapse analysis of receptor binding under modified chemical environments. Thirdly, the unbinding or rupture force F_R of the molecular pair is measured directly and can be related to binding affinities that characterize ligand binding kinetics. For the disciplines of biophysics and biological engineering as well as the pharmaceutical industry, this nanoscale functional mapping

of molecular interactions enables access to drug mechanisms, comparison of binding affinities among several candidate ligands, and even identification of previously unknown receptors. This approach is particularly well suited to consideration of ligands that are not amenable to conventional (fluorophore or radioactive isotope) labeling and of receptors with relatively low spatial density and mobility. Certainly, the rates of lateral diffusion and internalization of receptors within the cell membrane must be considered with respect to experimentally attainable scanning rates and resolutions. Nanomechanical imaging cannot easily distinguish a single feature that moves with timescales commensurate with the scanning rate from multiple features that do not move, and therefore interpretation of images demonstrating ligand-receptor interactions on living cell surfaces requires particular caution. We do not discuss all of the ligand-cell surface receptor pairs reported to date, but highlight different nanomechanical approaches that demonstrate the specificity of drug-cell interactions.

Key considerations in such experiments include validation of probe functionalization to ensure that the tethered ligand is present and oriented such that it can actively bind its receptor^{49,50}; accurate characterization of the cantilever spring constant k_c to convert deflection δ to force $F = k_c\delta$ ^{51,52,53}; and demonstration of binding specificity through, for example, competitive binding that eliminates measurable F_R with the soluble ligand⁵⁴ or ion-dependent disruption of receptor binding⁵⁵. Quantification of the ligand-receptor unbinding or rupture force F_R has been impressively demonstrated for a large number of proteins, with one tethered to the cantilevered probe and the other adhered to rigid substrata such as mica and Au^{7,50,56-70}. Of greater relevance to drug-cell interactions, F_R has also been reported between probe-bound ligands and receptors presented by cells that are typically^{16,64,71-74} but not always^{54,75,76} chemically fixed. Such ligand-receptor interactions on rigid surfaces or cell membranes were initially acquired 'blindly.' That is, ligand-receptor interrogation consisted of either acquisition of many $F - d$ responses at individual, randomly selected or topographically interesting sites, with no corresponding image of receptor distribution; or acquisition of single $F - d$ responses at each of many pixels comprising an image as in Fig. 1b providing a pixelated image of strong binding regions that were considerably larger than individual receptors. This approach is amenable to all custom-built and commercial AFMs, but does not afford mapping of the ligand-receptor interactions with molecular-scale spatial resolution (pixel size larger than hundreds of nanometers) and suffers from low throughput that is insufficient for rapid cell responses. Alternatively, for the ~ 10 nm-scale amplitude typical of magnetically driven oscillation³, deconvolution of the amplitude maxima and minima provides image contrast arising from strong probe-sample binding (recognition image) and sample topography (height image), respectively. The molecular resolution of this direct-binding approach, termed recognition imaging, has been demonstrated for several molecular pairs on rigid

surfaces^{7,56,77-82}. As shown in Fig. 9 for vascular endothelial cells, the approach provides the potential to image both the receptor distribution and to gather robust ligand-receptor F_R distributions on cell surfaces.

The extent to which the magnitude of F_R depends on the ligand-receptor pair, the experimental parameters employed, and the mechanical compliance of the receptor-presenting surface remain open and important questions that are currently being investigated through computational simulations such as steered molecular dynamics⁵⁹⁻⁶¹. For molecules adhered to rigid substrates including chemically fixed cells, F_R is on the order of 50 pN to 1000 pN (a distribution depending in large part on loading rate, as established through Bell's theorem¹⁰). This dependence of F_R distribution on experimental parameters can be used

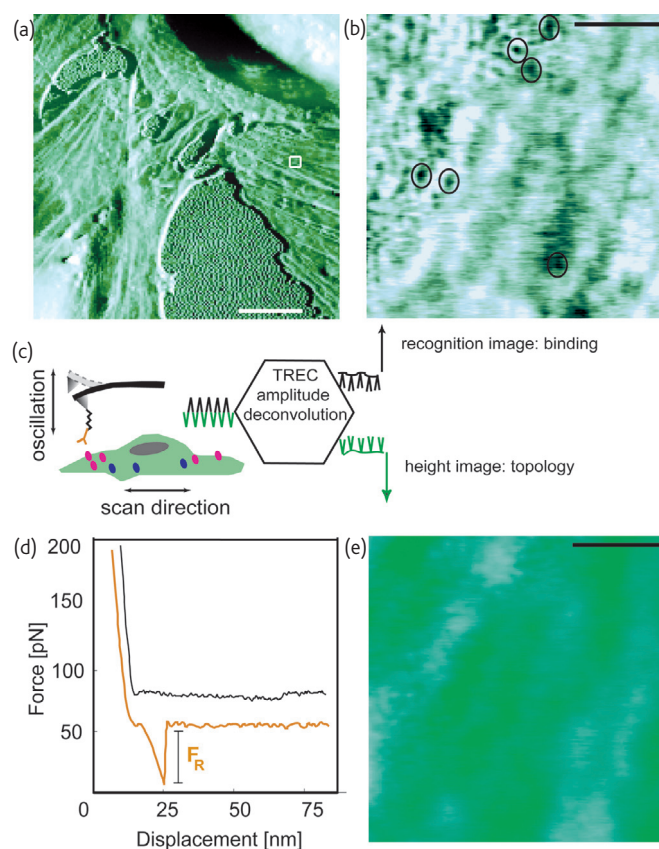


Fig. 9 Imaging of receptor distribution and ligand/antibody binding on intact cells. (a) Height or topography image of human umbilical vein endothelial cell region in magnetically actuated oscillation mode (MAC). Scalebar = 20 μm . (b) Cantilever deflection during oscillation of a ligand or antibody-functionalized probe can be deconvolved into a recognition image, where image contrast is a function of probe-surface binding (c), and a topography image (d). Scalebars = 500 nm. This deconvolution scheme is termed TREC[®]. Specificity of this binding is demonstrated through competitive inhibition of soluble ligands/antibodies, and changes in binding to or in response to drugs are imaged directly. The rupture force F_R between the functionalized probe and cell surface can also be measured pointwise to construct spatially coarse maps of receptor presence (orange) or absence (black), or to compare binding avidity in response to drugs. (Parts (a), (b), (d), and (e) are courtesy of S. Lee and K. J. Van Vliet, Massachusetts Institute of Technology. Part (c) adapted from⁵⁶. Reprinted with permission. © 2006 Nature Publishing Group.)

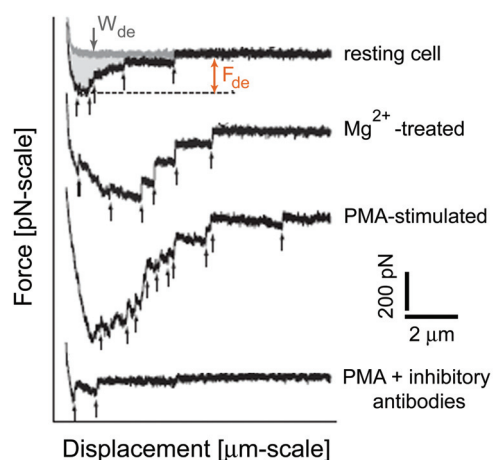


Fig. 10 Adhesion between whole cells and ligand-functionalized rigid surfaces can be explored in the presence of drugs to interpret mechanisms of action. Here, the drug phorbol myristate acetate (PMA) is demonstrated to increase the number of interactions between a cell bound to a cantilevered probe and an intercellular adhesion molecule (ICAM)-functionalized surface and to increase the corresponding work of de-adhesion W_{de} , but not to affect the quantum of force between the cell surface and this ligand. Disruption of the ICAM receptor via addition of Mg^{2+} and disruption of ICAM signaling via addition of inhibitory antibodies mitigate this enhanced adhesion in different ways. Cell mechanical compliance also increased with increased cell-ligand adhesion. (Reprinted with permission from⁸⁶. © 2003 The Company of Biologists.)

advantageously to estimate the energy landscape and kinetic quantities governing this interaction. For example, the rate of dissociation between the molecules k_{off} is inversely proportional to the time required to achieve F_R at a given applied force, as demonstrated for the Ca^{2+} -dependency of cadherin-cadherin binding⁵⁵. Such kinetic constants define the speed, specificity, and strength of drug-receptor interactions, while other complementary experimental approaches such as surface plasmon resonance do not provide access to single molecule analysis⁵⁸.

By adhering whole cells to AFM cantilevers, the ligand-receptor interactions governing adhesion between probe-bound and rigid surface-

bound ligands or whole cells can be considered at the single-cell level⁸³⁻⁸⁷. Although such experiments do not quantify receptor distribution or binding kinetics between individual ligand-receptor pairs, the drug-susceptibility of such intracellular adhesive interactions are key to pathological processes such as adhesion of cancer cells to endothelial cell-lined capillaries during metastasis. By quantifying the work of de-adhesion W_{de} directly from the $F-d$ response, it has been demonstrated that phorbol myristate acetate enhances the adhesion of leukocytes to monolayers of vascular endothelial intercellular adhesion molecules (ICAMs) by increasing the number of cancer cell receptors, but not the F_R between those receptors and ICAMs (Fig. 10)⁸⁶. In contrast, adhesion of leukocytes to adherent endothelial cell monolayers is increased significantly by the stimulation of endothelial cells by tumor necrosis factor- α (Fig. 11), and these mechanisms can be considered together by comparing W_{de} at endothelial cell-cell junctions with that at cell bodies⁸³. Liu *et al.*⁸⁵ have applied this whole cell approach to molecular-level adhesion in the search for novel antibiotics that prevent bacterial adhesion to surfaces. They found that the anecdotal prevention of bacterial infections via cranberry juice is not supported by a reduction in adhesion forces between *E. coli* bacteria and inorganic materials in the presence of this acidic media.

Summary

Applications and modifications of AFM provide the capacity to simultaneously map the structure and chemomechanical interactions of whole cells, membranes, and individual molecular receptors at or below the nanoscale. This enables systematic, *in situ* characterization of the mechanisms governing drug-cell interactions at the *in vitro* level. Although the near-molecular image resolution and single-molecule interaction force resolution of these approaches are impressive, it is important to note several current limitations of this contact-based approach for efficient discovery of new pharmaceutical solutions and understanding of existing mechanisms of drug action. These include restriction to two-dimensional, *in vitro* cell culture environments; low

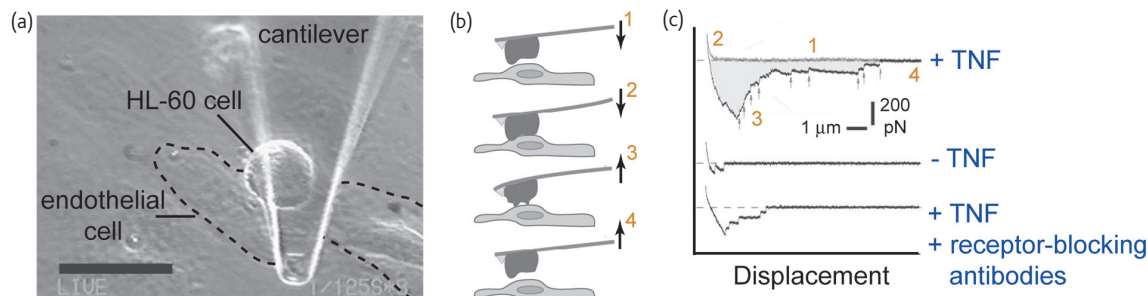



Fig. 11 Cell-cell adhesion can be modulated by drugs and measured through direct force-displacement responses. (a) A human promyelocytic leukemia (HL-60) cell adsorbed to a silicon nitride cantilever is positioned over a human umbilical vein endothelial cell monolayer, e.g. at cell-cell junctions. (b) The force-displacement response during adhesion and de-adhesion is acquired. (c) The work of de-adhesion (shaded) is increased when endothelial cells are stimulated by tumor necrosis factor- α (TNF), and reduced when cell-cell adhesion receptors are blocked by antibody binding. Adhesion between cancer and endothelial cells is required in metastasis, and such studies enable testing of drugs to mitigate this interaction. (Adapted from⁸³. Reprinted with permission. © 2004 American Physiological Society.)

throughput relative to the timescale of many cell responses (e.g. translational diffusion of receptors along membranes) and to the variability among cells within a population; and the potential to induce confounding cell responses by mechanical perturbing of the cell surface and its receptors. As these important current constraints are recognized and addressed through experimental and computational innovations, it is expected that this dynamic nanomechanical mapping of ligand-receptor interactions at the single-cell level will be key to scientific

advances in understanding, identifying, and developing therapies that promote human health. 

Acknowledgments

KJVW gratefully acknowledges the support of the US National Science Foundation Nanoscale Exploratory Research program and the Arnold and Mabel Beckman Foundation Young Investigator Program. PH acknowledges the support of the Austrian National Science Fund and the Austrian Nano and GENAU initiative from the Austrian Ministry of Education, Science and Culture.

REFERENCES

- Binnig, G., et al., *Phys. Rev. Lett.* (1986) **56**, 930
- Haberle, W., et al., *J. Vac. Sci. Technol. B* (1991) **9**, 1210
- Leuba, S. H., and Lindsay, S. M., *Biophys. J.* (1998) **74**, A71
- Couturier, G., et al., *J. Phys. D: Appl. Phys* (2001) **34**, 1266
- Erts, D., et al., *J. Phys. Chem. B* (2003) **107**, 3591
- Benmouna, F., et al., *Langmuir* (2003) **19**, 10247
- Kienberger, F., et al., *Acc. Chem. Res.* (2006) **39**, 29
- Sato, M., et al., *J. Biomech.* (2000) **33**, 127
- Sugawara, M., et al., *Hear. Res.* (2002) **174**, 222
- Bell, G. I., *Science* (1978) **200**, 618
- Bonfiglio, A., et al., *Exp. Cell Res.* (1995) **216**, 73
- Bushell, G. R. et al., *Cytometry* (1999) **36**, 254
- Wu, H. W., et al., *Scanning* (1998) **20**, 389
- Braet, F., et al., *J. Electron Microsc.* (2001) **50**, 283
- Rotsch, C. and Radmacher, M., *Biophys. J.* (2000) **78**, 520
- Charras, G. T. and Horton, M. A., *Biophys. J.* (2002) **82**, 2970
- Zhu, Y. J., et al., *FASEB J.* (2000) **14**, 1244
- Barboza, J. M. et al., *Arch. Androl.* (2004) **50**, 121
- Rotsch, C., et al., *Ultramicroscopy* (2001) **86**, 97
- Thompson, M. T., et al., *Biomaterials* (2005) **26**, 6836
- Schneider, S. W., et al., *Pflugers Arch.* (2000) **439**, 297
- Oberleithner, H., et al., *J. Membr. Biol.* (2003) **196**, 163
- Oberleithner, H., *Kidney Int.* (2005) **67**, 1680
- Schneider, S. W., et al., *Cell Biol. Int.* (1997) **21**, 759
- Anderson, R. C., et al., *FEMS Microbiol. Lett.* (2004) **240**, 105
- Braga, P. C., et al., *J. Chemother.* (2002) **14**, 336
- da Silva, Jr., A., and Teschke, O., *Biochim. Biophys. Acta.* (2003) **1643**, 95
- Meincken, M., et al., *Antimicrob. Agents Chemother.* (2005) **49**, 4085
- Thomas, W. E., et al., *Mol. Microbiol.* (2004) **53**, 1545
- Thomas, W., et al., *Biophys. J.* (2006) **90**, 753
- Pelling, A. E., et al., *Science* (2004) **305**, 1147
- Ji, X. L., et al., *World J. Gastroenterol.* (2005) **11**, 1709
- Cheng, Y., et al., *Biochim. Biophys. Acta.* (1999) **1421**, 249
- Girasole, M., et al., *J. Microsc.* (2001) **204**, 46
- Ruozi, B., et al., *J. Drug Target* (2003) **11**, 407
- Almofiti, M. R., et al., *Arch. Biochem. Biophys.* (2003) **410**, 246
- Vu, T. Q., et al., *Nano Lett.* (2005) **5**, 603
- Ruozi, B., et al., *J. Drug Target* (2005) **13**, 295
- Kawaura, C., et al., *FEBS Lett.* (1998) **421**, 69
- Zhao, L., and Feng, S. S., *J. Colloid Interface Sci.* (2006), in press
- Oishi, J., et al., *J. Control Release* (2006) **110**, 431
- Anabousi, S., et al., *Eur. J. Pharm. Biopharm.* (2005) **60**, 295
- Shahin, V., et al., *J. Cell Physiol.* (2005) **202**, 591
- Oberleithner, H., et al., *Pflugers Arch.* (2000) **439**, 251
- Oberleithner, H., et al., *Proc. Natl. Acad. Sci. USA* (1994) **91**, 9784
- Hong, S., et al., *Bioconjug. Chem.* (2004) **15**, 774
- Berquand, A., et al., *Pharm. Res.* (2005) **22**, 465
- Berquand, A., et al., *Biochim. Biophys. Acta.* (2004) **1664**, 198
- Klein, D. C. G., et al., *Chemphyschem.* (2003) **4**, 1367
- Riener, C. K., et al., *Anal. Chim. Acta.* (2003) **497**, 101
- Cleveland, J. P., et al., *Rev. Sci. Instrum.* (1993) **64**, 403
- Baumgartner, W., et al., *Ultramicroscopy* (2000) **82**, 85
- Hinterdorfer, P., et al., *Proc. Natl. Acad. Sci. USA* (1996) **93**, 3477
- Chen, A., and Moy, V. T., *Biophys. J.* (2000) **78**, 2814
- Baumgartner, W., et al., *Proc. Natl. Acad. Sci. USA* (2000) **97**, 4005
- Hinterdorfer, P., and Dufrene, Y. F., *Nat. Methods* (2006) **3**, 347
- Kienberger, F., et al., *Single Molecules* (2001) **2**, 99
- Gamsjaeger, R., et al., *Langmuir* (2004) **20**, 5885
- Raible, M., et al., *J. Biotechnol.* (2004) **112**, 13
- Evstigneev, M. and Reimann, P., *Phys. Rev. E.* (2003) **68**, 045103
- Pierres, A., et al., *Proc. Natl. Acad. Sci. Unit. States Am.* (1998) **95**, 9256
- Zhang, X. H., et al., *Chemphyschem.* (2004) **5**, 175
- Zhang, X. H., and Moy, V. T., *Biophys. Chem.* (2003) **104**, 271
- Zhang, X. H., et al., *Biophys. J.* (2002) **83**, 2270
- Yuan, C. B., et al., *Biochemistry* (2000) **39**, 10219
- Wong, J., et al., *Biomol. Eng.* (1999) **16**, 45
- Micic, M., et al., *Scanning* (1999) **21**, 394
- Eibl, R. H., and Moy, V. T., *Methods Mol. Biol.* (2005) **305**, 439
- Zhang, X., and Moy, V. T., *Biophys. Chem.* (2003) **104**, 271
- Yuan, C., et al., *Biochemistry* (2000) **39**, 10219
- Pfister, G., et al., *J. Cell Sci.* (2005) **118**, 1587
- Lee, S., and Van Vliet, K. J., (2006), unpublished results
- Van Vliet, K. J., et al., *Acta. Mater.* (2003) **51**, 5881
- Trache, A., et al., *Biophys. J.* (2005) **89**, 2888
- Horton, M., et al., *J. Recept. Signal Transduct. Res.* (2002) **22**, 169
- Lundberg, P., et al., *Endocrinology* (2001) **142**, 339
- Riener, C. K., et al., *Anal. Chim. Acta.* (2003) **479**, 59
- Kada, G., et al., *Ultramicroscopy* (2001) **86**, 129
- Stroh, C. M., et al., *Biophys. J.* (2004) **87**, 1981
- Stroh, C. M., et al., *Proc. Natl. Acad. Sci. USA* (2004) **101**, 12503
- Ebner, A., et al., *ChemPhysChem.* (2005), **6**, 897
- Hinterdorfer, P., *Methods Cell Biol.* (2002) **68**, 115
- Zhang, X., et al., *Am. J. Physiol. Heart Circ. Physiol.* (2004) **286**, H359
- Pouliot, J. M., et al., *Biomacromolecules* (2005) **6**, 1122
- Liu, Y., et al., *Biotechnol. Bioeng.* (2006) **93**, 297
- Wojcikiewicz, E. P., et al., *J. Cell Sci.* (2003) **116**, 2531
- Edmondson, K. E., et al., *Biophys. J.* (2005) **89**, 3603